

## THROMBOSIS AND HEMOSTASIS

Identification of extant vertebrate *Myxine glutinosa* VWF: evolutionary conservation of primary hemostasis

Marianne A. Grant,<sup>1,2</sup> David L. Beeler,<sup>1</sup> Katherine C. Spokes,<sup>1</sup> Junmei Chen,<sup>3</sup> Harita Dharaneeswaran,<sup>1</sup> Tracey E. Sciuto,<sup>4</sup> Ann M. Dvorak,<sup>4</sup> Gianluca Interlandi,<sup>5</sup> José A. Lopez,<sup>3</sup> and William C. Aird<sup>1,2</sup>

<sup>1</sup>Center for Vascular Biology Research, Department of Medicine, Beth Israel Deaconess Medical Center, Boston, MA; <sup>2</sup>Mount Desert Island Biological Laboratory, Salisbury Cove, ME; <sup>3</sup>Bloodworks Research Institute, University of Washington, Seattle, WA; <sup>4</sup>Department of Pathology, Beth Israel Deaconess Medical Center, Boston, MA; and <sup>5</sup>Department of Bioengineering, University of Washington, Seattle, WA

## Key Points

- The extant vertebrate hagfish, *M glutinosa*, has a single, functional *vwf* gene, structurally simpler than in higher vertebrates.
- VWF appeared in an ancestral vertebrate as a hemostatic protein lacking functional domains required for primary hemostasis under high flow.

Hemostasis in vertebrates involves both a cellular and a protein component. Previous studies in jawless vertebrates (cyclostomes) suggest that the protein response, which involves thrombin-catalyzed conversion of a soluble plasma protein, fibrinogen, into a polymeric fibrin clot, is conserved in all vertebrates. However, similar data are lacking for the cellular response, which in gnathostomes is regulated by von Willebrand factor (VWF), a glycoprotein that mediates the adhesion of platelets to the subendothelial matrix of injured blood vessels. To gain evolutionary insights into the cellular phase of coagulation, we asked whether a functional *vwf* gene is present in the Atlantic hagfish, *Myxine glutinosa*. We found a single *vwf* transcript that encodes a simpler protein compared with higher vertebrates, the most striking difference being the absence of an A3 domain, which otherwise binds collagen under high-flow conditions. Immunohistochemical analyses of hagfish tissues and blood revealed Vwf expression in endothelial cells and thrombocytes. Electron microscopic studies of hagfish tissues demonstrated the presence of Weibel-Palade bodies in the endothelium. Hagfish Vwf formed high-molecular-weight multimers in hagfish plasma and in stably transfected CHO cells. In

functional assays, botrocetin promoted VWF-dependent thrombocyte aggregation. A search for *vwf* sequences in the genome of sea squirts, the closest invertebrate relatives of hagfish, failed to reveal evidence of an intact *vwf* gene. Together, our findings suggest that VWF evolved in the ancestral vertebrate following the divergence of the urochordates some 500 million years ago and that it acquired increasing complexity through sequential insertion of functional modules. (*Blood*. 2017;130(23):2548-2558)

## Introduction

von Willebrand factor (VWF) is a large multimeric glycoprotein expressed in endothelial cells and megakaryocytes/platelets (reviewed in Denis, Ruggeri, Sadler, and Haberichter and Montgomery<sup>1-4</sup>). VWF mediates the adhesion and aggregation of platelets at sites of vascular injury (reviewed in Lenting et al, Mendolicchio and Ruggeri, and Reininger<sup>5-7</sup>). Normally, globular VWF binds collagen in the subendothelial matrix following vascular injury. Collagen binding, together with shear stress, enables VWF to assume an extended conformation, resulting in exposure of its A1 domain, which can then interact with GPIIb/IIIa on the surface of platelets. In addition, VWF binds and transports coagulation factor VIII (FVIII), thereby protecting FVIII from rapid clearance and increasing its half-life.<sup>8-10</sup> Deficient or defective VWF results in von Willebrand disease (VWD), a common inherited bleeding disorder, whereas overactive VWF has been implicated in several thrombotic disorders, including thrombotic thrombocytopenic purpura.<sup>11</sup>

In humans, VWF is synthesized as a precursor protein of 2813 amino acids with a cleavable 22-amino-acid signal peptide, a large 741-amino-acid propeptide (VWF antigen II), and a mature

multidomain subunit of 2050 amino acids (Figure 1A) (reviewed in Lenting et al<sup>12</sup>). After removal of the signal peptide, the 307-kDa monomer (pro-VWF) undergoes posttranslational modification with the addition of up to 22 carbohydrate chains, and assembles in the endoplasmic reticulum into dimers through disulfide bonds between C-terminal cysteine knot (CTCK) domains (at VWF Cys2771, Cys2773, and Cys2811).<sup>13</sup> Pro-VWF dimers are then transported to the Golgi, where furin-mediated cleavage of the propeptide occurs after the D1-D2 domains. The remaining N-terminal D3 domain undergoes additional head-to-head interdisulfide bonding at Cys1142 and Cys1099, leading to multimerization of VWF.<sup>14</sup> The number of subunits in each multimer varies, with molecular weights ranging from 500 000 (mature VWF dimer) to >20 million Daltons.

Megakaryocyte-derived VWF is stored in platelet  $\alpha$ -granules.<sup>15</sup> In endothelial cells, VWF directs the formation of its own releasable storage granule, the Weibel-Palade body (WPB),<sup>16</sup> through a multistep process that generates and packages highly active, high-molecular-weight VWF multimers in a heliocoid structure or tubule (reviewed in Nightingale and Cutler, Sadler, and Valentijn et al<sup>17-19</sup>). Once released,

Submitted 26 February 2017; accepted 23 August 2017. Prepublished online as *Blood* First Edition paper, 12 September 2017; DOI 10.1182/blood-2017-02-770792.

The online version of this article contains a data supplement.

The publication costs of this article were defrayed in part by page charge payment. Therefore, and solely to indicate this fact, this article is hereby marked "advertisement" in accordance with 18 USC section 1734.

© 2017 by The American Society of Hematology



all terminal procedures, hagfish were anesthetized in seawater containing tricaine methanesulfonate (MS-222; 1:2500 wt/vol) prior to decapitation. Experimental procedures were approved by the Animal Care and Use Committee at the Mount Desert Island Biological Laboratory. The supplemental Materials and methods, available on the *Blood* Web site, include the isolation of the hagfish *vwf* gene, the stable transfection of Chinese hamster ovary (CHO) cells, the generation of antibodies against hagfish Vwf, quantitative real-time polymerase chain reaction (qPCR) assays, histochemistry and immunohistochemistry, western blots, agarose gel plasma VWF multimer analysis, optical platelet aggregation studies, ADAMTS13 cleavage of CHO cell-expressed hagfish VWF, electron microscopy, protein sequence analysis, homology protein structure modeling, and A2 model structure tensile force-induced unfolding simulations.

## Results

### Cloning and characterization of hagfish *vwf* cDNA

To clone full-length *vwf* cDNA from hagfish, we used PCR with degenerate primers (supplemental Table 1) designed from conserved amino acid regions within multiple vertebrate VWF sequence alignments, followed by rapid amplification of cDNA ends using gene-specific and nested primer sets (supplemental Table 1). The 6513-bp open reading frame encodes a putative protein of 2170 amino acids (237.5 kDa). Processing of a putative N-terminal 15-amino-acid signal sequence would result in a predicted protein (pro-Vwf) of 2155 amino acids (235.9 kDa). Further processing to remove the 740-amino-acid propeptide sequence would result in a mature protein (mature-Vwf) of 1415 amino acids (155.2 kDa). Hagfish pro-Vwf is 636 amino acids shorter than human with 31.5% overall sequence homology (supplemental Table 2). Alignments of hagfish Vwf to VWF sequences from multiple vertebrates, ranging from pufferfish to humans (supplemental Figure 1-2A-E; supplemental Table 3), identify the conservation of specific domains in hagfish Vwf and the absence of other domains that are otherwise conserved in higher vertebrates. Based on recently revised domain annotations of VWF,<sup>28</sup> hagfish Vwf contains VWD1-C8-1-TIL-1-E1, VWD2-C8-2-TIL-2-E2, TIL'-E', VWD3-C8-3-TIL-3-E3, A1, A2, C2-C6, and CTCK (Figure 1A). The FVIII binding region, the GPIIb $\alpha$  binding region, and the GPIIb/IIIa binding region are each intact. Interestingly, hagfish Vwf is missing A3, D4N, VWD4-C8-4-TIL-4, and C1. In mammals, the function of the C-terminal C1-C6 domains remains poorly understood. However, the absence of A3 suggests that hagfish Vwf does not bind to collagen types I and III, whereas the lack of a D4 domain raises the possibility that ADAMTS13-Vwf docking does not occur in hagfish.

Other key features of hagfish Vwf are identifiable with varying degrees of conservation. The furin propeptide cleavage site Rx(R/K)R is highly conserved in all species examined (Figure 1B), and in hagfish, comprises the same extended SxRxKRSLxC sequence as in human,<sup>36</sup> suggesting that the propeptide of hagfish Vwf is cleaved by furin. The putative site for Vwf-cleaving protease ADAMTS13 in the A2 domain, based on sequence alignment, comprises an F-L residue pair. Although this differs from the highly conserved Y-M cleavage sequence observed in amphibians, birds, reptiles, and mammals (Figure 1C), it is consistent with the F-L pair observed in virtually all fish studied to date (except coelacanth, a fish more closely related to lobe-finned fish and tetrapods than common ray-finned fishes, which has an F-M residue pair). Finally, the CTCK cysteine residues involved in dimerization of pro-VWF (VWF Cys2771, Cys 2773, and Cys2811) and the D3 domain cysteine residues (Cys1142 and Cys1099) required for head-to-head interdisulfide bonding and multimerization of VWF are highly conserved (supplemental Figure 2B,E).

### Hagfish *vwf* is expressed as a single gene product

To determine if the cloned *vwf* cDNA represents the only expressed *vwf* mRNA transcript in hagfish, we first carried out low-temperature annealing PCR using primers complementary to a region within the A2 domain region or an A2 through C2-C3 intervening loop region (supplemental Table 1). Analysis of PCR products amplified from hagfish heart, liver, gill, and skin cDNA showed single products of the expected size for both primer pairs (Figure 2A). Next, we carried out Northern blot hybridization of hagfish RNA from heart and gill with probes spanning portions of the A1-A2 region or the 3' untranslated region of hagfish *vwf* (primer pairs used in PCR to generate DNA probes given in supplemental Table 1). These experiments revealed a single 7.5-kb transcript in both heart and gill (Figure 2B). Together, these findings argue against the presence of a duplicate *vwf* gene (or pseudogene) in hagfish.

### Hagfish Vwf is expressed in endothelium and peripheral blood

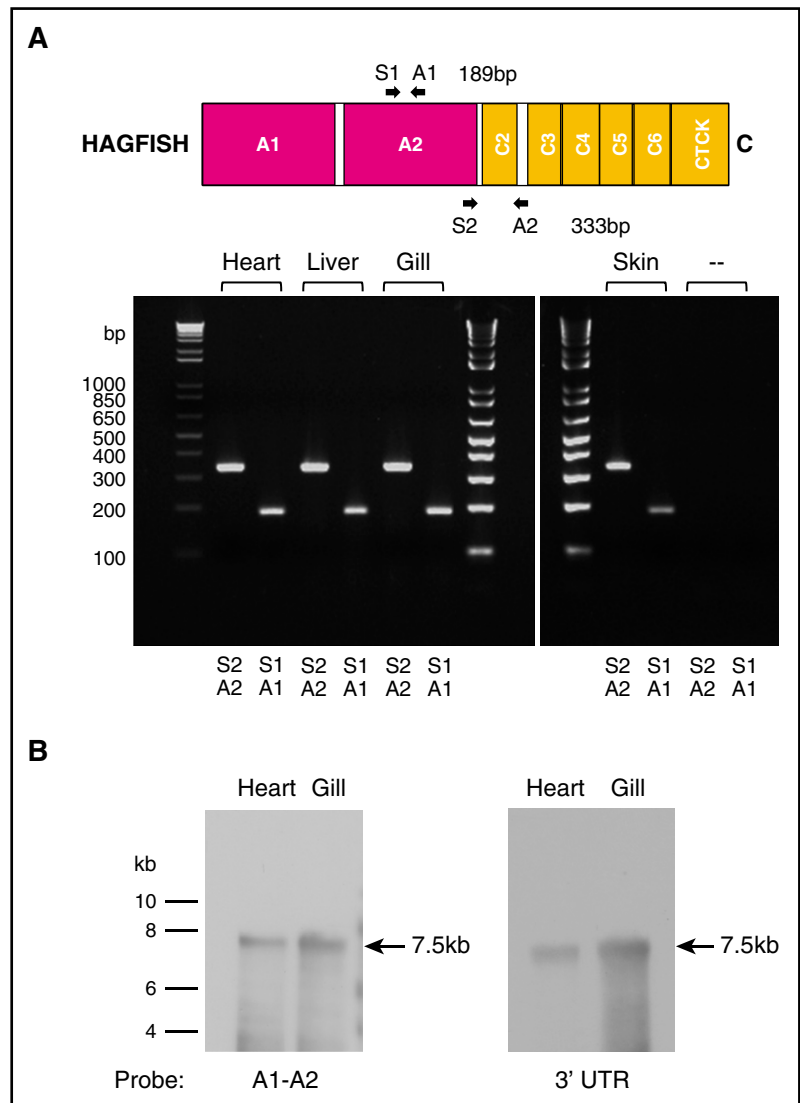
qPCR analysis of various hagfish tissues and whole blood revealed widespread expression of *vwf* mRNA, with highest transcript levels in the aorta and liver (Figure 3A). To localize Vwf expression, we carried out immunofluorescent studies. We began by testing the reactivity and specificity of a series of anti-human VWF antibodies. Remarkably, a human polyclonal antibody from Dako (A0082), which is reported to have cross-reactivity with several mammalian VWFs as well as that of chicken, revealed a positive signal in the endothelium of multiple hagfish organs (Figure 3B; supplemental Figure 3A). To validate these results, we generated a mouse monoclonal anti-hagfish antibody (B10). Staining of tissue sections revealed a pattern identical to that observed with the Dako antibody (supplemental Figure 3B). In contrast to its mammalian counterpart, which is heterogeneously distributed across the vascular tree,<sup>37</sup> hagfish Vwf was detected throughout all blood vessels examined.

In hagfish peripheral blood smears, immunofluorescence showed staining of Vwf in a subpopulation of nucleated blood cells (Figure 3C), whose morphology is consistent with thrombocytes as previously described by others (see supplemental Results and supplemental Figure 4 for description of hagfish blood cells).<sup>38</sup> The staining demonstrated a punctate pattern, suggesting that Vwf may be stored in cytoplasmic granules. To confirm that hagfish thrombocytes do indeed possess granules, we carried out electron microscopy of peripheral blood. We identified a population of cells whose morphology is clearly distinct from that of erythrocytes and granulocytes and similar to that described for thrombocytes in fish.<sup>39</sup> These cells contained a single type of granule throughout the cytoplasm (supplemental Figure 5). Together, our results suggest that expression of VWF in endothelial cells and platelets is evolutionarily conserved in all vertebrates.

### Hagfish Vwf is localized in endothelial WPBs

In higher vertebrates, VWF is stored in endothelial WPBs.<sup>19</sup> We previously demonstrated that hagfish endothelial cells contain WPBs.<sup>40</sup> Here, we carried out additional electron microscopic studies of hagfish tissues and confirmed the presence of WPBs in the intact endothelium (Figure 4A aorta; Figure 4B skeletal muscle arteriole). In en face preparations of the aorta, confocal immunofluorescence revealed punctate staining in all endothelial cells, consistent with localization of Vwf in WPBs (Figure 4C). Thus, storage of VWF in WPB appears to be an evolutionarily conserved feature of endothelial VWF processing.

**Figure 2. Hagfish *vwf* is expressed as a single gene product.** (A) PCR primer pairs A1/S1 and A2/S2 (supplemental Table 1) were used to generate DNA products from the A2 domain or from a region of the A2 domain to the C2-C3 spacer from hagfish *vwf* cDNA prepared by reverse transcription from hagfish heart, liver, gill, and skin RNA. Only the expected 189-bp and 333-bp PCR products were observed on agarose gel analysis. (–) Control reactions without template cDNA. (B) Northern blot hybridization of hagfish RNA from heart and gill with probes that spanned either the A1-A2 region or the 3' untranslated region (UTR) from the hagfish *vwf* gene (supplemental Table 1). A single 7.5-kb transcript is observed in both heart and gill.



**Hagfish Vwf propeptide undergoes posttranslational processing**

We next examined the expression and posttranslational processing of Vwf in hagfish heart lysates and plasma by sodium dodecyl sulfate-polyacrylamide gel electrophoresis (SDS-PAGE) and western blot analysis with anti-Vwf antibody. Bands observed correlated with the expected size of unprocessed hagfish Vwf (pro-Vwf) at ~240 kDa, as well as mature Vwf at ~165 kDa (Figure 5A). Similar analyses using cell lysates from mouse heart showed unprocessed mouse VWF (pro-VWF) at ~300 kDa and mature VWF at ~250 kDa (Figure 5A). These results suggest conservation in the processing of mature VWF by posttranslational cleavage of the propeptide sequence.

**Hagfish Vwf forms mid-sized multimers in plasma**

In mammals, VWF circulates in plasma as large, multimeric forms. To determine whether hagfish Vwf exhibits a similar pattern, we carried out nonreducing agarose gel analysis of plasma samples from hagfish, mice, and humans, followed by western blotting. In hagfish, the smallest band was ~330 kDa, likely representing the dimerized form of Vwf (Figure 5B). Consistent with the abbreviated size of hagfish Vwf, this product was visibly smaller than the lowest-sized VWF multimers

in human and mouse plasmas. Similar to its mouse and human counterparts, hagfish plasma demonstrated a ladder of Vwf multimers, although it lacked the higher-molecular-weight multimers (>7 bands) observed in human and mouse.

**Hagfish Vwf is cleaved by human ADAMTS13**

In mammals, ADAMTS13 cleaves the single bond between Y and M (human residues 1605 and 1606) located in the A2 domain.<sup>41</sup> ADAMTS13 cleavage requires partial unfolding of the VWF multimer either naturally by shear stress or artificially by chemical denaturation.<sup>42</sup> To determine whether ADAMTS13 cleaves hagfish Vwf, we chemically denatured hagfish Vwf from whole-cell lysates of stably transfected CHO cells (generation of these clones is discussed in more detail below) with 1.5 M urea and incubated it with full-length (aa 34-1427) recombinant human ADAMTS13. Cleavage was assessed on reducing SDS-PAGE gels and detected by western blotting. As shown in Figure 5C, addition of human ADAMTS13 in the absence but not presence of EDTA resulted in significant cleavage of hagfish Vwf concomitant with the appearance of a C-terminal cleavage product (~61 kDa), strongly suggesting conservation of a functional cleavage site in hagfish Vwf.

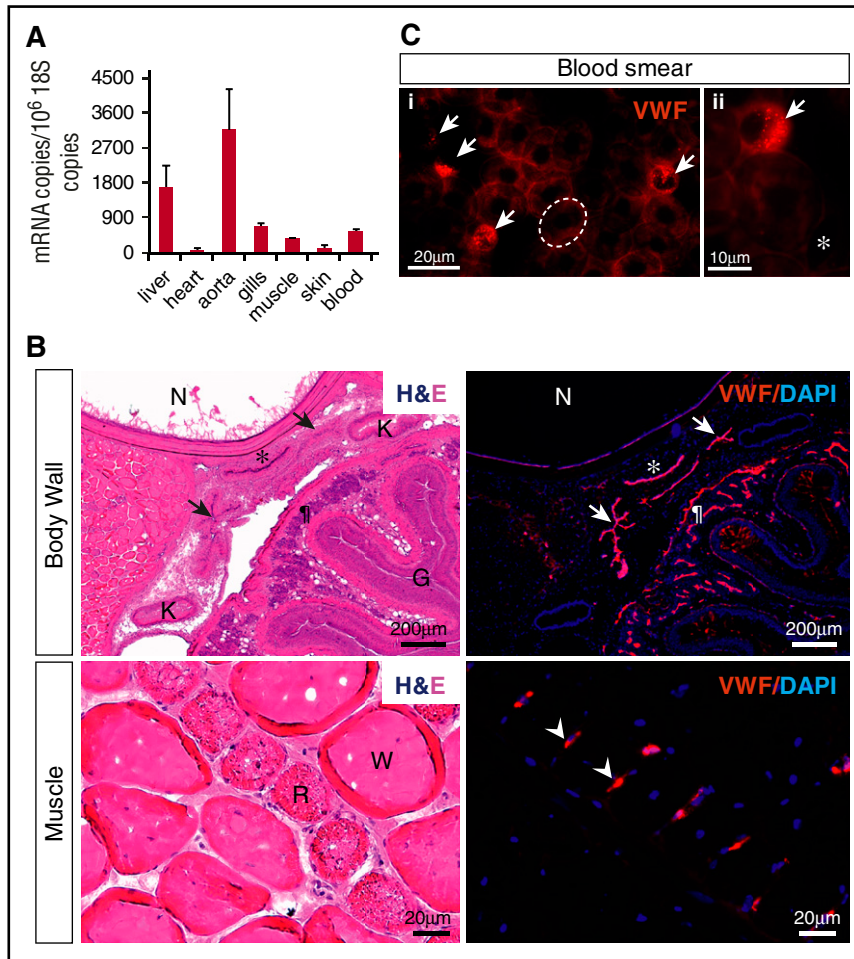


**Figure 3. Hagfish Vwf is expressed in endothelium and peripheral blood.** (A) qPCR analysis of hemostatic factors in hagfish organs and blood. mRNA expression is represented as copy number per  $10^6$  18S copies. Data are presented as mean  $\pm$  standard deviation (SD) ( $n = 3$  fish). (B) Serial sections of the body wall and muscle of hagfish stained with hematoxylin and eosin (H&E) (left) and processed for immunofluorescence staining using polyclonal anti-human VWF antibody (right). Nuclei are stained with 4',6-diamidino-2-phenylindole (DAPI). Positive Vwf staining is observed in the aorta (\*), posterior cardinal veins (arrows), capillaries of the intestinal wall (¶), and capillaries surrounding red muscle fibers (arrowheads). All stain and magnification information for photomicrographs is provided in the supplemental Material. G, gut lumen; K, kidney; N, notochord; R, red muscle fiber; W, white muscle fiber. (C) Fluorescence microscopy images of hagfish blood processed for immunofluorescence staining of Vwf using polyclonal anti-human VWF antibody. Left image (i) shows 4 Vwf-positive cells (arrows), which are smaller than neighboring Vwf-negative erythrocytes (1 of these is outlined in white). Right image (ii) is a higher-power view showing the punctate staining pattern of a Vwf-positive cell surrounded by Vwf-negative erythrocytes and spindle cells. All stain and magnification information for photomicrographs is provided in the supplemental Material. \*Representative spindle cell. See supplemental Figure 4C-D for greater detail of negatively stained cells.

### Hagfish thrombocyte agglutination elicited by botrocetin

To test whether hagfish Vwf is functional, we employed optical aggregometry of hagfish thrombocytes. Ristocetin is typically used to test for human VWF-mediated platelet aggregation. However, ristocetin does not agglutinate mouse platelets,<sup>43,44</sup> and in our studies, ristocetin failed to agglutinate hagfish thrombocytes (not shown). Botrocetin, a component of *Bothrops jararaca* venom, has been shown to induce platelet agglutination by a VWF-dependent mechanism that involves binding to GPIIb/IIIa receptors on platelets.<sup>45</sup> The addition of botrocetin resulted in a dose-dependent aggregation of hagfish thrombocytes in the presence but not absence of hagfish plasma (Figure 5D; supplemental Figure 6). These findings suggest that hagfish Vwf binds to a GPIIb/IIIa-like receptor on hagfish thrombocytes and is functionally active.

### Heterologously expressed hagfish Vwf in CHO cells forms Vwf multimers

To establish whether the cloned gene product undergoes processing and multimerization, we stably transfected CHO cells with full-length hagfish *vwf*. Although CHO cells lack a pathway for regulated secretion, they have previously been shown to cleave pro-vWF and generate high-molecular-weight multimers.<sup>46-48</sup> Clones were selected in puromycin-containing culture medium, and hagfish Vwf expression was verified by qPCR (Figure 6A). Cell lysates were subjected to reducing or nonreducing SDS-PAGE followed by western blot analysis using monoclonal anti-hagfish antibody (Figure 6B). Under reducing

conditions, 2 major bands were detected that correlated with unprocessed hagfish Vwf (pro-Vwf) at  $\sim 240$  kDa and processed mature Vwf at  $\sim 165$  kDa. Western blots of nonreducing gels demonstrated the presence of bands consistent with Vwf dimer and tetramer (Figure 6B). Immunofluorescence of the stably transfected clones with either anti-human or anti-hagfish antibodies revealed cytoplasmic staining (Figure 6C) in a pattern similar to that previously described for heterologously expressed human VWF in CHO cells.<sup>48,49</sup> In electron microscopic studies, large membrane-bound organelles containing flocculent, electron-dense material were observed in CHO cells expressing hagfish Vwf (Figure 6D). These structures, which resemble dilated endoplasmic reticulum, were not present in untransfected cells or in control cells expressing hagfish tissue factor pathway inhibitor. In summary, cloned hagfish Vwf expressed in CHO cells undergoes cleavage of the pro-Vwf to generate the mature subunit and undergoes partial multimerization.

### Structures of the A domains of hagfish VWF by homology modeling

Structural models of VWF A domains are important tools for investigations into sequence and structure relationships, including potential ligand binding and ADAMTS13 cleavage. With that in mind, we carried out homology modeling of hagfish Vwf A1 and A2 domains. Similar to previously determined human or murine VWF A domain structures,<sup>50-53</sup> hagfish Vwf A1 and A2 each demonstrated VWA  $\alpha/\beta$  folds, with a  $\beta$ -sheet core composed of 6  $\beta$ -strands encircled by a series

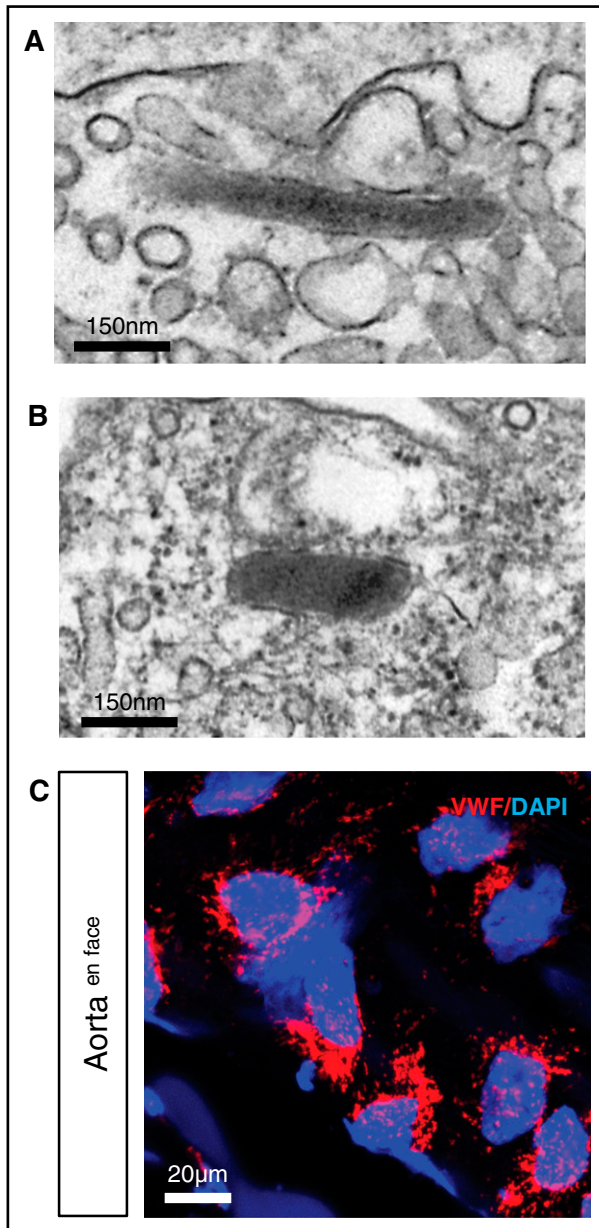


**Figure 4. Punctate Vwf staining and presence of WPBs in hagfish endothelial cells.** Representative electron microscopy image of hagfish endothelium from aorta (A) and skeletal muscle arteriole (B) showing the presence of cigar-shaped organelles containing electron-dense tubules, consistent with WPBs. (C) Confocal laser scanning microscopy image of en face hagfish aorta processed for immunofluorescence staining of Vwf using polyclonal anti-human VWF antibody (see supplemental Figure 3 for images using hagfish monoclonal Vwf antibody). Nuclei are stained with DAPI. Note the presence of punctate staining in the endothelial cells. All stain and magnification information for photomicrographs is provided in the supplemental Material.

of  $\alpha$ -helices (Figure 7). The A1 homology structure showed a main chain root mean squared deviation of 0.875 Å over 191 aligned residues with 27% sequence identity (supplemental Table 2) to experimentally determined human A1 (PDB ID 1AUQ). The A2 homology structure showed a main chain root mean squared deviation of 0.477 Å over 164 aligned residues with 30% sequence identity (supplemental Table 2) to experimentally determined human VWF A2 (PDB ID 3ZQK) (Figure 7). The ADAMTS13 cleavage site from hagfish Vwf (F1611 and L1612) superimposes on its human counterpart (Y1605 and M1606) in the  $\beta$ 4-strand.

### Reduced tensile force requirement for hagfish A2 domain unfolding

The application of tensile force leads to unfolding of the A2 domain and exposure of the ADAMTS13 cleavage site. Previous molecular dynamics (MD) simulations with human A2 demonstrated that force-induced unfolding begins at the C-terminus and proceeds with secondary structure elements sequentially unfolding.<sup>54,55</sup> Separation of the C-terminal helix  $\alpha$ 6 from the rest of A2 and exposure of a “C-terminal hydrophobic core” located near A1661 constitutes a major rate-limiting step. Because hagfish have extremely low blood pressures, we hypothesized that hagfish A2 would demonstrate less stability and enhanced susceptibility to ADAMTS13 than human A2. Indeed, similar MD simulations carried out with modeled hagfish A2 suggested that a conserved C-terminal hydrophobic core in hagfish Vwf A2 was partially exposed in the absence of force and required a lower tensile force to expose the C-terminal hydrophobic core and initiate unfolding of A2 compared with its human counterpart (supplemental Figures 7-8).

### A search of *Ciona* genomes does not reveal evidence of a Vwf gene

To determine whether Vwf is expressed in the closest invertebrate relatives of hagfish, we searched available sequences from sea squirt *Ciona intestinalis* (database version 82.3/assembly GCA\_000224145.1) and *Ciona savignyi* (database version 82.2/draft assembly CSAV2.0) using BLAST tools for protein sequence and domain similarity to hagfish Vwf. Search of *C intestinalis* yielded 17 hits, the most similar being a “Vwf-like” gene that lacks all A domains, the D4N domain, and C-terminal domains corresponding to C2-C4 (supplemental Figure 9), and furthermore, contains large sequence insertions in multiple regions that have no known similarities. Search of *C savignyi* revealed 19 hits, with 2 showing similarity to hagfish Vwf (supplemental Figure 9). One sequence (SAV2) aligns only with the N-terminal 3 VWD regions and beyond that shares no sequence or domain structure with vertebrate VWF. The second sequence (SAV1) has the greatest alignment and domain conservation to hagfish Vwf. It contains 3 sequential A domains, 1 D domain (VWD-C8-TIL), and 3 additional incomplete D domains (containing C8-TIL-E, VWD-C8, VWD-C8 modules, respectively). The furin cleavage site is not conserved. The C-terminal domain differs from vertebrate VWF in lacking repeats of cysteine-rich C-domain sequences. Interestingly, cysteine residues that mediate interchain disulfide bond dimerization (Cys1099, Cys1142, Cys2771, and Cys 2773) are conserved between human VWF and SAV1. Together with the absence of a closed circulatory system and thrombocytes in urochordates, these findings argue against the presence of a functional VWF in these organisms.

## Discussion

Hagfish and lamprey (cyclostomes), referred to as agnathans or jawless fish, lack a hinged jaw, and their skeleton is not mineralized. They are the sole survivors of the agnathan stage in vertebrate evolution and are the closest extant outgroups to all jawed vertebrates (gnathostomes). Their immediate nonvertebrate relatives are the Urochordata (tunicates) and Cephalochordata (amphioxus). The last common ancestor of hagfish and jawed vertebrates (cartilaginous fish [chondrichthyes] and the bony fishes [osteichthyes], amphibians, reptiles, birds, and mammals) was also the last common ancestor of all extant vertebrates. Features that are shared between hagfish and gnathostomes can be

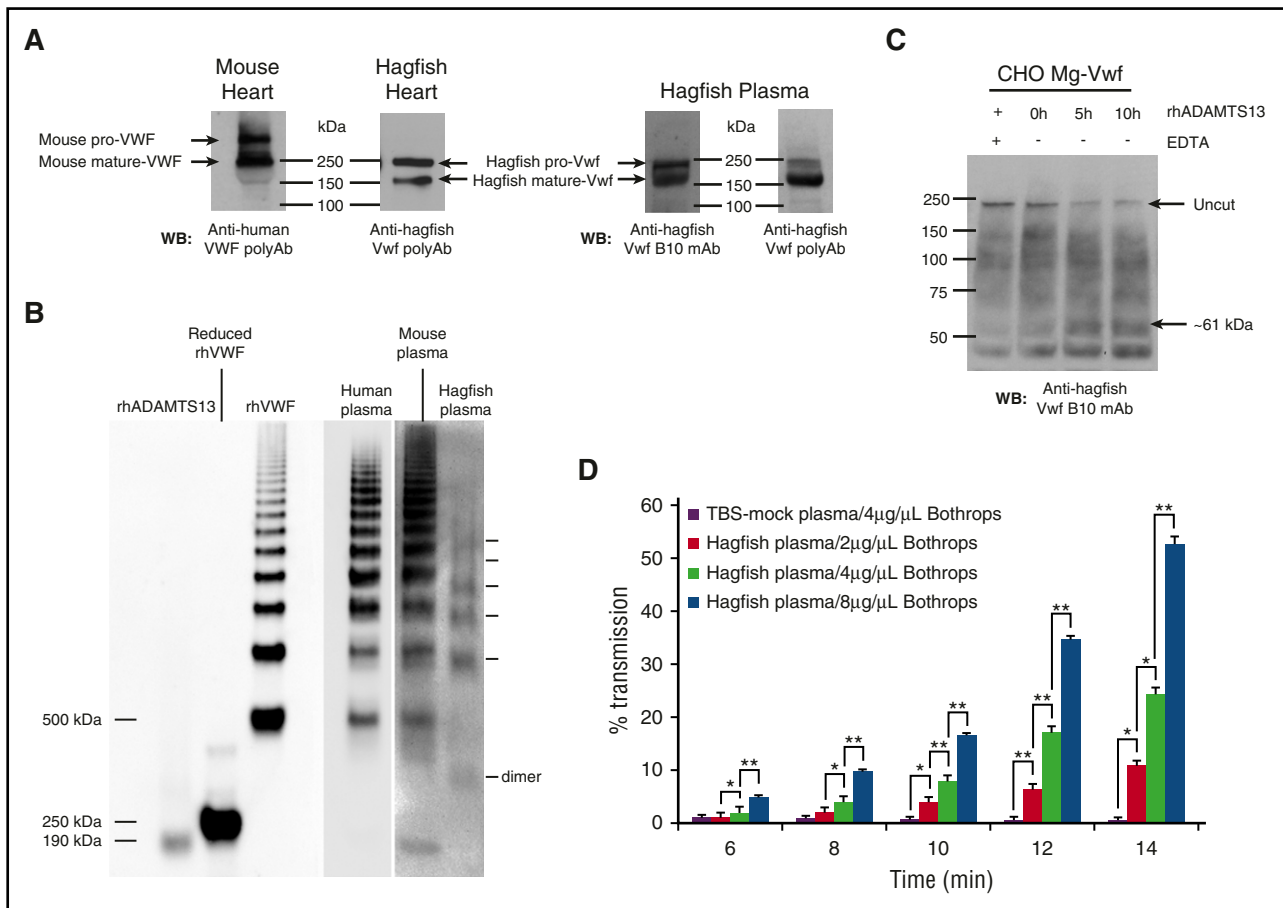


**Figure 5. Hagfish Vwf processing, plasma multimers, ADAMTS13 cleavage, and platelet aggregation.** (A) Western blot (WB) of heart lysates from mouse or hagfish using polyclonal anti-human VWF antibody (Dako) or monoclonal anti-hagfish VWF antibody (B10), and of hagfish plasma using either monoclonal anti-hagfish Vwf antibody (B10) or polyclonal anti-hagfish Vwf antibody. Shown are bands whose sizes are consistent with mouse pro-VWF (~300 kDa) and mature VWF (~250 kDa), or hagfish pro-VWF (~240 kDa) and mature VWF (~165 kDa). (B) Human, mouse, and hagfish plasma proteins were separated on a nonreducing 1.5% agarose gel. Western blotting was carried out with polyclonal anti-human VWF antibody (Dako) alongside molecular weight marking samples of reduced and nonreduced recombinant human VWF (rhVWF) and recombinant human ADAMTS13 (rhADAMTS13). (C) Samples of hagfish Vwf from expressing CHO-cell lysates in 1.5 M urea buffer were incubated for up to 10 hours with 70 nM of full-length recombinant human ADAMTS13 with (+) or without (-) 15 mM EDTA. Note the significant reduction of the ~240-kDa pro-Vwf band in the presence of ADAMTS13 and the appearance of a C-terminal cleavage product (~61 kDa) detected with monoclonal anti-hagfish B10 antibody raised against C-terminal Vwf sequence. (D) Thrombocyte-rich and thrombocyte-poor plasma were prepared from ~12 hagfish animals and measured for thrombocyte aggregation as measured by light transmission over time. Thrombocytes resuspended in thrombocyte-poor plasma were equilibrated for 2 minutes at 37°C with stirring and then incubated with varying concentrations of botrocetin (*B jararaca* snake venom). Thrombocyte agglutination was monitored over time (reported as minutes following addition of botrocetin) using a dual-channel optical aggregometer. Data represent the mean and SD from 3 independent experiments. Statistical analysis was carried out using paired Student *t* test (\**P* ≤ .5; \*\**P* ≤ .005). polyAB, polyclonal antibody; TBS, Tris-buffered saline; WB, western blot.

inferred to have already been present in this ancestral vertebrate. We have shown that hagfish, like jawed vertebrates (gnathostomes), express a functional Vwf. Our search of Ciona databases failed to reveal compelling evidence of Vwf in urochordates. These findings suggest that Vwf evolved following the divergence of urochordates from the vertebrate lineage, >500 million years ago.

Several features of hagfish Vwf are shared with its mammalian counterpart. For example, hagfish Vwf is expressed both in endothelial cells and in a subpopulation of nucleated peripheral blood cells consistent with thrombocytes. In addition, hagfish endothelium possesses WPBs, as evidenced by our electron microscopy studies. The punctate staining of Vwf in hagfish endothelium suggests that the protein is packaged and stored in these organelles. By extension, these data suggest that the release of Vwf from hagfish endothelial cells is regulated, at least in part, by an inducible pathway, as it is in humans and mice.

In mammals, VWF is differentially expressed between and within different vascular beds.<sup>37</sup> For example, VWF is undetectable in liver sinusoidal endothelial cells of the mouse and demonstrates patchy expression in capillaries of the heart and in the aorta. In contrast, hagfish

Vwf was detected throughout the endothelium of all vascular beds examined, including the aorta. Although definitive proof for ubiquitous expression would require colocalization studies with a pan-endothelial marker (which to our knowledge is not available for hagfish), our findings suggest that vascular bed-specific expression of VWF evolved following the divergence of hagfish. We recently demonstrated that VWF expression in mice is regulated by a bistable switch whose state-switching dynamics vary across the vascular tree.<sup>56</sup> The finding that hagfish Vwf is expressed in all endothelial cells suggests that expression is locked into a single ON state and is impervious to the effects of biological noise or organ-specific extracellular cues.

Similar to higher vertebrates, hagfish Vwf circulates in a multimerized form. Interestingly, hagfish plasma demonstrated smaller multimers compared with humans. Previous studies of mammalian VWF have shown that the hemostatic function of VWF, including its binding to collagen and GPIIb/IIIa, decreases as the multimer size decreases.<sup>57</sup> Presumably, the reduced multimer size in hagfish is sufficient to mediate thrombocyte-subendothelial interactions in these animals. We also demonstrated that hagfish Vwf has a

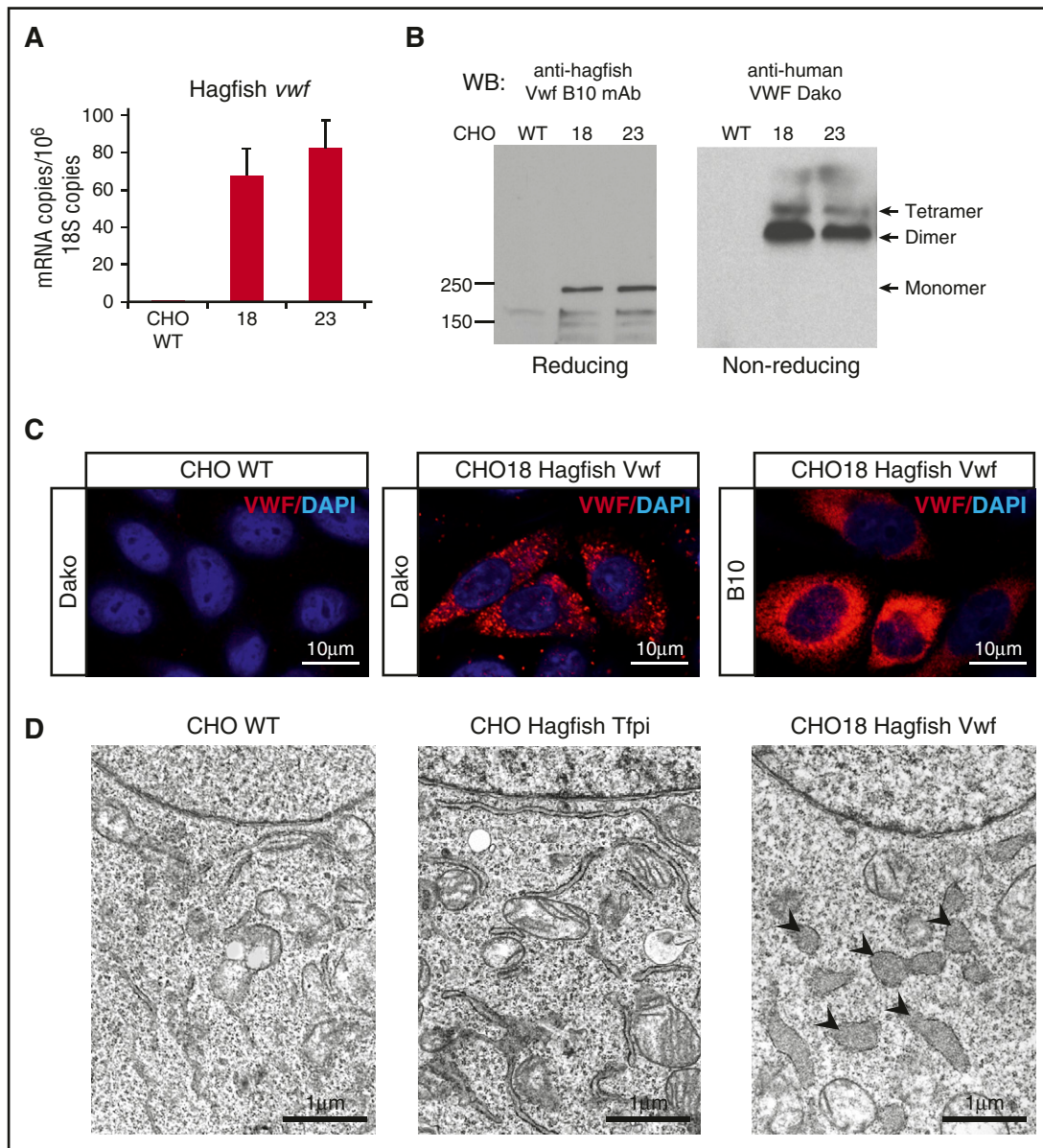


**Figure 6. Hagfish VWF forms multimers in mammalian cell culture.** (A) qPCR analysis of hagfish *vwf* in untransfected CHO cells (CHO WT) and CHO cells stably transfected with hagfish *vwf* (clones 18 and 23). mRNA expression is represented as copy number per 10<sup>6</sup> 18S copies. Data are presented as mean  $\pm$  SD (n = 3 fish). (B) Heterologous expression of hagfish Vwf in CHO cell culture visualized by western blotting of whole-cell lysates on reducing or nonreducing SDS-PAGE with B10 anti-hagfish mAb or Dako anti-human pAb, as indicated. (C) Representative confocal laser scanning microscopy images of control CHO cells (CHO WT) or CHO cells stably transfected with hagfish Vwf (CHO18 Hagfish Vwf) processed for staining of Vwf using polyclonal anti-human VWF antibody (Dako) or monoclonal anti-hagfish Vwf antibody (B10). All stain and magnification information for photomicrographs is provided in the supplemental Material. (D) Electron micrographs of control CHO cells (CHO WT) and CHO cells expressing hagfish tissue factor pathway inhibitor (CHO Hagfish Tfpi) or hagfish Vwf (CHO18 Hagfish Vwf). Nucleus appears at the top of each cell. Note the large irregularly shaped organelles (arrowheads) in the Vwf-expressing cells which contain electron dense material.

partially conserved ADAMTS13 cleavage site and is cleaved by human ADAMTS13. Thus, it likely that hagfish Vwf is not only secreted as a high-molecular-weight multimer, but that its size is regulated by an ADAMTS13-like protease.

Hagfish Vwf contains a highly conserved GPIIb $\alpha$  binding site in the A1 domain. Previous studies in mammals have shown that A1 binds GPIIb $\alpha$  under conditions of high shear stress at sites of vascular injury.<sup>58,59</sup> A recent study employing MD simulations, atomic force microscopy, and microfluidic experiments demonstrated that the human VWF A2 domain normally blocks the GPIIb $\alpha$ -binding site in A1.<sup>60</sup> This autoinhibition was relieved when VWF was exposed to a stretching force (mimicking shear stress), resulting in A2 domain

unfolding prior to ADAMTS13-mediated cleavage. In our simulations, we found that compared with human, the C-terminal helix of hagfish A2 requires a lower force to be undocked. Hagfish have the lowest blood pressures of all vertebrates, with systolic pressures in the dorsal aorta measuring a mere 5.8 to 9.8 mm Hg.<sup>61</sup> Thus, it is interesting to speculate that a lower threshold for force-mediated reversal of the A2-A1 interaction is adapted to low-flow conditions. Similarly, our MD simulations suggested that the C-terminal hydrophobic core is partially exposed in hagfish A2, which may explain why the threshold for force-mediated unfolding is lower in hagfish compared with human VWF. This property would not only facilitate thrombocyte binding under low-flow conditions, but would also enhance ADAMTS13



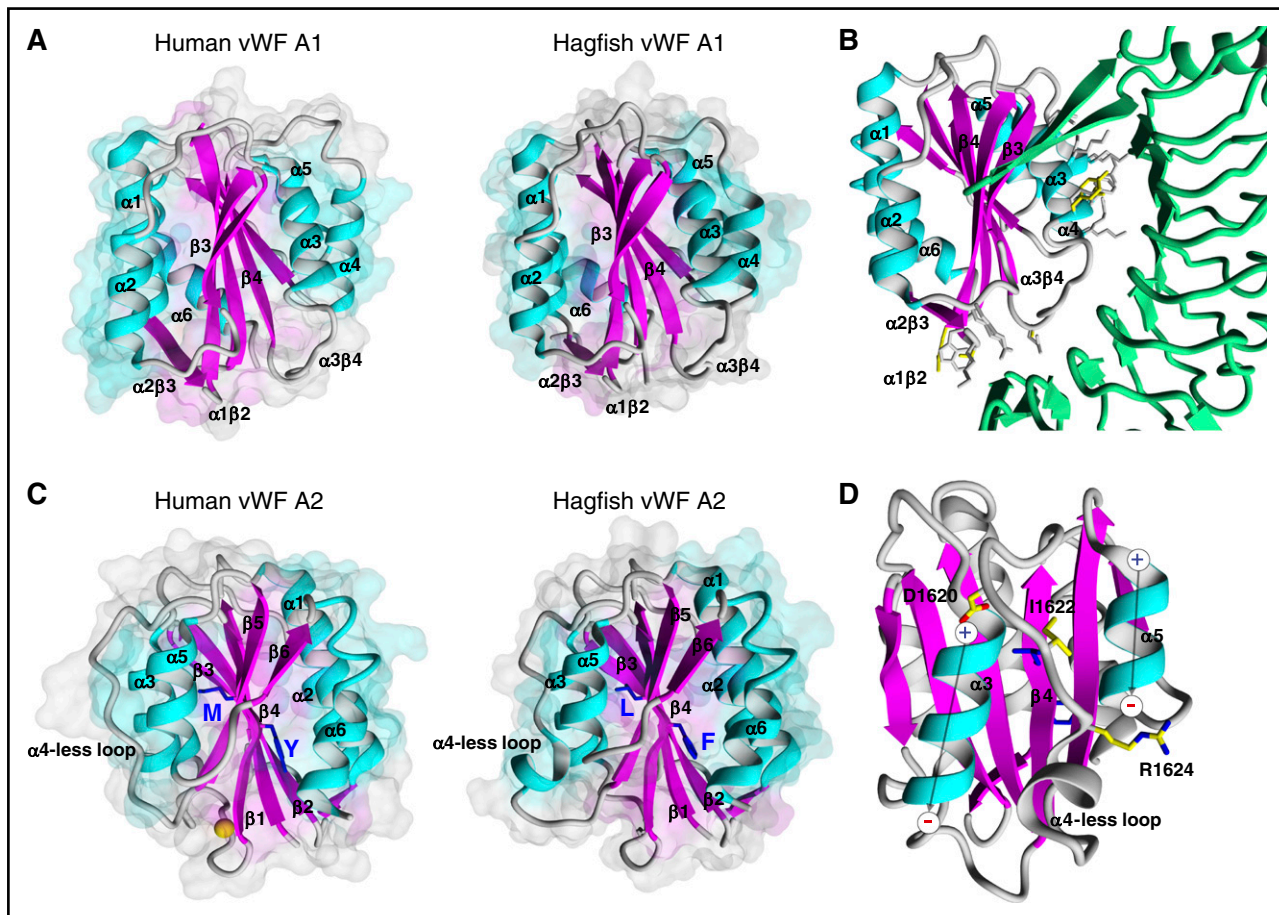


**Figure 7. Hagfish VWF A1 and A2 domain structures.** (A) Comparative model of hagfish A1 (backbone ribbon representation on surface volume renderings) in comparison with the experimentally determined human A1 structure (PDB ID 1AUQ). The structures are highly superimposable with the exception of  $\alpha 4$ , where hagfish is truncated by 4 residues, similar to known bird, amphibian, and fish sequences, impacting the length of the helix and  $\beta 4\alpha 4$  loop conformation. (B) Superimposition of the hagfish A1 onto experimentally determined human A1 bound to GPIIb $\alpha$  (green ribbon) (PDB ID 3SQ0). The many amino acids shown to contribute to the GPIIb $\alpha$  binding interface that are conserved in hagfish A1 are highlighted (gray sticks) along with those few not conserved in hagfish A1 (yellow sticks). In addition, charge is conserved between hagfish and human among 5 of the 7 electrostatically charged residues, as is the hydrophobic character of 3 of 4 residues. (C) Comparative model structure of hagfish A2 in comparison with the experimentally determined human A2 structure (PDB ID 3ZQK). Like human, hagfish A2 is distinguished from other VWA domains by a relatively long unstructured loop at helix 4 ( $\alpha 4$ ). (D) Modeling of the  $\alpha 4$ -less loop environment in hagfish A2. The  $\alpha 3$ - and  $\alpha 5$ -helix dipole moments are symbolized. The strictly conserved buried hydrophobic I1622 side chain atoms, and D1620 N-cap and R1624 C-cap side chain atoms are shown (yellow sticks). Although the hagfish  $\alpha 4$ -less region contains 5 additional residues compared with human, the  $\alpha 4$ -less loop environment is well conserved.

cleavage of Vwf, perhaps contributing to the relatively narrow spectrum of multimers observed in hagfish plasma.

A remarkable finding in the present study is that the hagfish *vwf* gene lacks certain domains critical for VWF function in higher vertebrates. Most notable is the absence of the A3 domain which suggests that hagfish Vwf does not bind fibrillar collagen (types I and III). In humans, mutations that affect collagen binding in A3 are associated with a bleeding phenotype.<sup>62</sup> In contrast, hagfish Vwf A1 domain is conserved and likely mediates binding to collagen types IV and VI. Interestingly, previous studies have shown that VWF A3-collagen interactions occur only under conditions of high shear, whereas type VI collagen demonstrates VWF-dependent platelet binding under conditions of low shear.<sup>63</sup> vWF may have evolved in the ancestral vertebrate as a critical mediator of platelet adhesion to the subendothelial matrix under low-flow conditions, with the A3 domain appearing in later vertebrates as an adaptation to higher blood pressures and shear rates. An alternative explanation is that the A3 domain was lost in the hagfish lineage after its split from the other vertebrate lineages. Indeed, it is interesting to speculate that A3 domain loss is a derived feature of VWF in other vertebrates with extremely low blood pressures.

The carboxyl-terminal domains of VWF, D4-CTCK, are cysteine rich. A recent study demonstrated that the cysteine amino acids in the VWD4, C1, C5, C6 domains and N-terminus of the CTCK domain are important for the precise folding of C-terminal domains.<sup>64</sup> It was hypothesized that mutations eliminating these cysteine residues might influence dimeric bouquet formation and consequently helical assembly of tubules and storage. It is tempting to speculate that the absence in hagfish Vwf of D4N, VWD4-C8-4-TIL-4 (previously D4) and C1 (previously B1) helps explain the small size of hagfish Vwf multimers compared with mammals.

VWD and VWA domains have each been identified in protists, suggesting that they were early inventions during eukaryotic evolution.<sup>65,66</sup> VWD in combination with the C8 domain appears in choanoflagellates, whereas VWD domains containing 3 repeats of VWD-C8-TIL is first observed in ctenophores.<sup>66</sup> In vertebrates, the VWD-C8-TIL repeats combine with other domains to form mucins and nonmucin proteins, including VWF. The addition of a PTS domain is characteristic of mucins, whereas the addition of VWA is a hallmark of VWF. Indeed, the combination of VWD and VWA domains has not been previously identified in any other protein in vertebrates or *C. intestinalis*, leading others to conclude that VWF is unique to

vertebrates.<sup>67</sup> In our own bioinformatics search, we discovered a sequence in the *C savignyi* database that contains 1 complete and 3 incomplete D domains together with 3 tandem A domains. Because this combination has not been described in any other gene, we suggest that the A-D domain motif is orthologous, and that 1 of the A domains was lost in hagfish (1 event). A less parsimonious interpretation is that the ancestor had 2 A domains (retained in hagfish), and there have been 2 independent gains in *C savignyi* and gnathostomes (2 events). Alternatively, the ancestral gene had 3 A domains, 1 was lost in the ancestor of hagfish and gnathostomes, and a third A domain was gained in gnathostomes (2 events). In contrast to the striking homology of the A-D domain architecture, the predicted structure of the *C savignyi* protein lacks many of the key features of VWF, including C-terminal repeats of cysteine-rich C domains and is thus at best considered a partial ortholog of vertebrate VWF.

In summary, our findings suggest that VWF and primary hemostasis arose during a narrow window of time following the divergence of the urochordates from the ancestral vertebrate, and that it was initially adapted to a low-flow, low-pressure cardiovascular system. In future studies, it will be interesting to carry out structure-function relationships of hagfish Vwf and determine whether the gene is involved in processes other than primary hemostasis, including the binding of a factor V/VIII precursor.

## Acknowledgments

The authors gratefully acknowledge Lauren Janes, Beth Israel Deaconess Medical Center, for providing technical expertise; and

J. Evan Sadler, Washington University School of Medicine, St. Louis, Missouri, and David A. Haig, the Department of Organismic and Evolutionary Biology, Harvard University, for their valuable insights.

This research was supported in part by grants from the National Institutes of Health, National Heart, Lung, and Blood Institute (HL086766) (M.A.G.), (HL119322) (W.C.A.), (HL117639-01 and HL112633) (J.A.L.), and career development award (K25HL118137) (G.I.). Simulations were performed on the Comet supercomputer at the San Diego Supercomputing Center thanks to an XSEDE allocation (TG-MCB060069N) (G.I.), which is made available in part through National Science Foundation support.

## Authorship

Contribution: M.A.G. and W.C.A. conceived the study; M.A.G., D.L.B., K.C.S., J.C., H.D., T.E.S., and G.I. performed the experiments; M.A.G., W.C.A., A.M.D., and J.A.L. advised on experimental design and data analysis; M.A.G., W.C.A., and G.I. wrote the manuscript; and all authors contributed to the discussion of the data and critically reviewed and revised the manuscript.

Conflict-of-interest disclosure: The authors declare no competing financial interests.

Correspondence: Marianne A. Grant, Division of Cardiovascular Medicine, Department of Medicine, Center for Vascular Biology Research, Beth Israel Deaconess Medical Center, Harvard Medical School, Boston, MA 02215; e-mail: mgrant@bidmc.harvard.edu.

## References

1. Denis CV. Molecular and cellular biology of von Willebrand factor. *Int J Hematol*. 2002;75(1):3-8.
2. Ruggeri ZM. Structure of von Willebrand factor and its function in platelet adhesion and thrombus formation. *Best Pract Res Clin Haematol*. 2001; 14(2):257-279.
3. Sadler JE. Biochemistry and genetics of von Willebrand factor. *Annu Rev Biochem*. 1998;67: 395-424.
4. Habricher SL, Montgomery RR. Structure and Function of von Willebrand Factor. In: Marder VJ, Aird WC, Bennet JS, Schulman S, White GC, eds. Hemostasis and Thrombosis: Basic Principles and Clinical Practice. Philadelphia PA: Lippincott Williams & Wilkins; 2013:197-207.
5. Lenting PJ, Pegon JN, Groot E, de Groot PG. Regulation of von Willebrand factor-platelet interactions. *Thromb Haemost*. 2010;104(3): 449-455.
6. Mendolicchio GL, Ruggeri ZM. New perspectives on von Willebrand factor functions in hemostasis and thrombosis. *Semin Hematol*. 2005;42(1):5-14.
7. Reininger AJ. Function of von Willebrand factor in haemostasis and thrombosis. *Haemophilia*. 2008; 14(suppl 5):11-26.
8. Hoyer LW. The factor VIII complex: structure and function. *Blood*. 1981;58(1):1-13.
9. Nogami K, Shima M, Nishiya K, et al. A novel mechanism of factor VIII protection by von Willebrand factor from activated protein C-catalyzed inactivation. *Blood*. 2002;99(11): 3993-3998.
10. Weiss HJ, Sussman II, Hoyer LW. Stabilization of factor VIII in plasma by the von Willebrand factor. Studies on posttransfusion and dissociated factor VIII and in patients with von Willebrand's disease. *J Clin Invest*. 1977;60(2):390-404.
11. Budde U, Schneppenheim R. Interactions of von Willebrand factor and ADAMTS13 in von Willebrand disease and thrombotic thrombocytopenic purpura. *Hamostaseologie*. 2014;34(3):215-225.
12. Lenting PJ, Christophe OD, Denis CV. von Willebrand factor biosynthesis, secretion, and clearance: connecting the far ends. *Blood*. 2015; 125(13):2019-2028.
13. Katsumi A, Tuley EA, Bodó I, Sadler JE. Localization of disulfide bonds in the cystine knot domain of human von Willebrand factor. *J Biol Chem*. 2000;275(33):25585-25594.
14. Purvis AR, Gross J, Dang LT, et al. Two Cys residues essential for von Willebrand factor multimer assembly in the Golgi. *Proc Natl Acad Sci USA*. 2007;104(40):15647-15652.
15. Sporn LA, Chavin SI, Marder VJ, Wagner DD. Biosynthesis of von Willebrand protein by human megakaryocytes. *J Clin Invest*. 1985;76(3): 1102-1106.
16. Wagner DD. The Weibel-Palade body: the storage granule for von Willebrand factor and P-selectin. *Thromb Haemost*. 1993;70(1): 105-110.
17. Nightingale T, Cutler D. The secretion of von Willebrand factor from endothelial cells; an increasingly complicated story. *J Thromb Haemost*. 2013;11(suppl 1):192-201.
18. Sadler JE. von Willebrand factor assembly and secretion. *J Thromb Haemost*. 2009;7(suppl 1): 24-27.
19. Valentijn KM, Sadler JE, Valentijn JA, Voorberg J, Eikenboom J. Functional architecture of Weibel-Palade bodies. *Blood*. 2011;117(19):5033-5043.
20. Zander CB, Cao W, Zheng XL. ADAMTS13 and von Willebrand factor interactions. *Curr Opin Hematol*. 2015;22(5):452-459.
21. Flood VH, Gill JC, Christopherson PA, et al. Critical von Willebrand factor A1 domain residues influence type VI collagen binding. *J Thromb Haemost*. 2012;10(7):1417-1424.
22. Flood VH, Schlauderaff AC, Habricher SL, et al; Zimmerman Program Investigators. Crucial role for the VWF A1 domain in binding to type IV collagen. *Blood*. 2015;125(14):2297-2304.
23. Hoylaerts MF, Yamamoto H, Nuyts K, Vreys I, Deckmyn H, Vermynen J. von Willebrand factor binds to native collagen VI primarily via its A1 domain. *Biochem J*. 1997;324(Pt 1):185-191.
24. Kuo HJ, Maslen CL, Keene DR, Glanville RW. Type VI collagen anchors endothelial basement membranes by interacting with type IV collagen. *J Biol Chem*. 1997;272(42):26522-26529.
25. Pareti FI, Niiya K, McPherson JM, Ruggeri ZM. Isolation and characterization of two domains of human von Willebrand factor that interact with fibrillar collagen types I and III. *J Biol Chem*. 1987; 262(28):13835-13841.
26. Rand JH, Patel ND, Schwartz E, Zhou SL, Potter BJ. 150-kD von Willebrand factor binding protein extracted from human vascular subendothelium is type VI collagen. *J Clin Invest*. 1991;88(1): 253-259.
27. Ruggeri ZM. Platelet adhesion under flow. *Microcirculation*. 2009;16(1):58-83.
28. Zhou YF, Eng ET, Zhu J, Lu C, Walz T, Springer TA. Sequence and structure relationships within von Willebrand factor. *Blood*. 2012;120(2): 449-458.
29. Muia J, Zhu J, Gupta G, et al. Allosteric activation of ADAMTS13 by von Willebrand factor. *Proc Natl Acad Sci USA*. 2014;111(52):18584-18589.
30. South K, Luken BM, Crawley JT, et al. Conformational activation of ADAMTS13. *Proc Natl Acad Sci USA*. 2014;111(52):18578-18583.

31. Doolittle RF. The evolution of vertebrate blood coagulation: a case of Yin and Yang. *Thromb Haemost.* 1993;70(1):24-28.
32. Hanumanthaiah R, Day K, Jagadeeswaran P. Comprehensive analysis of blood coagulation pathways in teleostei: evolution of coagulation factor genes and identification of zebrafish factor VIII. *Blood Cells Mol Dis.* 2002;29(1):57-68.
33. Doolittle RF, Jiang Y, Nand J. Genomic evidence for a simpler clotting scheme in jawless vertebrates. *J Mol Evol.* 2008;66(2):185-196.
34. Chitta MS, Duhé RJ, Kermode JC. Cloning of the cDNA for murine von Willebrand factor and identification of orthologous genes reveals the extent of conservation among diverse species. *Platelets.* 2007;18(3):182-198.
35. Ghosh A, Vo A, Twiss BK, et al. Characterization of zebrafish von Willebrand factor reveals conservation of domain structure, multimerization, and intracellular storage. *Adv Hematol.* 2012; 2012:214209.
36. Rehemtulla A, Kaufman RJ. Preferred sequence requirements for cleavage of pro-von Willebrand factor by propeptide-processing enzymes. *Blood.* 1992;79(9):2349-2355.
37. Regan ER, Aird WC. Dynamical systems approach to endothelial heterogeneity. *Circ Res.* 2012;111(1):110-130.
38. Mattisson AGM, Fänge R. Light- and electronmicroscopic observations on the blood cells of the Atlantic hagfish, *Myxine glutinosa* (L.). *Acta Zoologica.* 1977;58(4):205-221.
39. Rowley AF, Ratcliffe NA, eds. *Vertebrate Blood Cells.* Cambridge, UK; New York, NY: Cambridge University Press; 1988.
40. Yano K, Gale D, Massberg S, et al. Phenotypic heterogeneity is an evolutionarily conserved feature of the endothelium. *Blood.* 2007;109(2): 613-615.
41. Furlan M, Robles R, Lämmle B. Partial purification and characterization of a protease from human plasma cleaving von Willebrand factor to fragments produced by in vivo proteolysis. *Blood.* 1996;87(10):4223-4234.
42. Tsai HM. Physiologic cleavage of von Willebrand factor by a plasma protease is dependent on its conformation and requires calcium ion. *Blood.* 1996;87(10):4235-4244.
43. Bergmeier W, Rackebbrandt K, Schröder W, Zirngibl H, Nieswandt B. Structural and functional characterization of the mouse von Willebrand factor receptor GPIb-IX with novel monoclonal antibodies. *Blood.* 2000;95(3):886-893.
44. Ware J, Russell S, Ruggeri ZM. Cloning of the murine platelet glycoprotein Ibalph gene highlighting species-specific platelet adhesion. *Blood Cells Mol Dis.* 1997;23(2):292-301.
45. Read MS, Smith SV, Lamb MA, Brinkhous KM. Role of botrocetin in platelet agglutination: formation of an activated complex of botrocetin and von Willebrand factor. *Blood.* 1989;74(3): 1031-1035.
46. Fischer B, Mitterer A, Schlokot U, DenBouwmeester R, Dörner F. Structural analysis of recombinant von Willebrand factor: identification of hetero- and homo-dimers. *FEBS Lett.* 1994;351(3):345-348.
47. Bonthron DT, Handin RI, Kaufman RJ, et al. Structure of pre-pro-von Willebrand factor and its expression in heterologous cells. *Nature.* 1986; 324(6094):270-273.
48. Wagner DD, Saffaripour S, Bonfanti R, et al. Induction of specific storage organelles by von Willebrand factor propolypeptide. *Cell.* 1991; 64(2):403-413.
49. Rosnoblet C, Ribba AS, Wollheim CB, Kruithof EK, Vischer UM. Regulated von Willebrand factor (vWf) secretion is restored by pro-vWf expression in a transfectable endothelial cell line. *Biochim Biophys Acta.* 2000;1495(1):112-119.
50. Emsley J, Cruz M, Handin R, Liddington R. Crystal structure of the von Willebrand Factor A1 domain and implications for the binding of platelet glycoprotein Ib. *J Biol Chem.* 1998;273(17): 10396-10401.
51. Zhang Q, Zhou YF, Zhang CZ, Zhang X, Lu C, Springer TA. Structural specializations of A2, a force-sensing domain in the ultralarge vascular protein von Willebrand factor. *Proc Natl Acad Sci USA.* 2009;106(23):9226-9231.
52. Zhou M, Dong X, Baldauf C, et al. A novel calcium-binding site of von Willebrand factor A2 domain regulates its cleavage by ADAMTS13. *Blood.* 2011;117(17):4623-4631.
53. Jakobi AJ, Mashaghi A, Tans SJ, Huizinga EG. Calcium modulates force sensing by the von Willebrand factor A2 domain. *Nat Commun.* 2011; 2:385.
54. Baldauf C, Schneppenheim R, Stacklies W, et al. Shear-induced unfolding activates von Willebrand factor A2 domain for proteolysis. *J Thromb Haemost.* 2009;7(12):2096-2105.
55. Interlandi G, Ling M, Tu AY, Chung DW, Thomas WE. Structural basis of type 2A von Willebrand disease investigated by molecular dynamics simulations and experiments. *PLoS One.* 2012; 7(10):e45207.
56. Yuan L, Chan GC, Beeler D, et al. A role of stochastic phenotype switching in generating mosaic endothelial cell heterogeneity. *Nat Commun.* 2016;7:10160.
57. Mikhail S, Aldin ES, Streiff M, Zeidan A. An update on type 2B von Willebrand disease. *Expert Rev Hematol.* 2014;7(2):217-231.
58. Dayananda KM, Singh I, Mondal N, Neelamegham S. von Willebrand factor self-association on platelet GpIbalpha under hydrodynamic shear: effect on shear-induced platelet activation. *Blood.* 2010;116(19): 3990-3998.
59. Miyata S, Ruggeri ZM. Distinct structural attributes regulating von Willebrand factor A1 domain interaction with platelet glycoprotein Ibalph under flow. *J Biol Chem.* 1999;274(10): 6586-6593.
60. Aponte-Santamaría C, Huck V, Posch S, et al. Force-sensitive autoinhibition of the von Willebrand factor is mediated by interdomain interactions. *Biophys J.* 2015;108(9):2312-2321.
61. Forster ME. The blood sinus system of hagfish: its significance in a low-pressure circulation. *Comp Biochem Physiol Part A Physiol.* 1997;116(3): 239-244.
62. Legendre P, Navarrete AM, Rayes J, et al. Mutations in the A3 domain of von Willebrand factor inducing combined qualitative and quantitative defects in the protein. *Blood.* 2013; 121(11):2135-2143.
63. Ross JM, McIntire LV, Moake JL, Rand JH. Platelet adhesion and aggregation on human type VI collagen surfaces under physiological flow conditions. *Blood.* 1995;85(7):1826-1835.
64. Yadegari H, Driesen J, Pavlova A, et al. Insights into pathological mechanisms of missense mutations in C-terminal domains of von Willebrand factor causing qualitative or quantitative von Willebrand disease. *Haematologica.* 2013;98(8):1315-1323.
65. Whittaker CA, Hynes RO. Distribution and evolution of von Willebrand/integrin A domains: widely dispersed domains with roles in cell adhesion and elsewhere. *Mol Biol Cell.* 2002; 13(10):3369-3387.
66. Lang T, Klasson S, Larsson E, Johansson ME, Hansson GC, Samuelsson T. Searching the evolutionary origin of epithelial mucus protein components-mucins and FCGBP. *Mol Biol Evol.* 2016;33(8):1921-1936.
67. Lang T, Hansson GC, Samuelsson T. Gel-forming mucins appeared early in metazoan evolution. *Proc Natl Acad Sci USA.* 2007;104(41): 16209-16214.